# Open Archive TOULOUSE Archive Ouverte (OATAO)

OATAO is an open access repository that collects the work of Toulouse researchers and makes it freely available over the web where possible.

This is an author-deposited version published in : http://oatao.univ-toulouse.fr/
Eprints ID : 4420

# Modeling soil moisture–reflectance

Etienne Muller[*], Henri Décamps

*Centre d'Ecologie des Systèmes Aquatiques Continentaux (CESAC), UMR C5576, CNRS, University Paul Sabatier, 29, rue Jeanne Marvig,
31055 Toulouse Cedex 4, France*

## Abstract

Spectral information on soil is not easily available as vegetation and farm works prevent direct observation of soil responses. However, there is an increasing need to include soil reflectance values in spectral unmixing algorithms or in classification approaches. In most cases, the impact of soil moisture on the reflectance is unknown and therefore ignored. The objective of this study was to model reflectance changes due to soil moisture in a real field situation using multiresolution airborne Spot data. As the direct observation of soils is only possible in the absence of vegetation, the effective remote sensing of soil moisture is limited to a few days each year. In such a favorable time window, modeling the soil moisture–reflectance relationships was found possible. The proposed exponential model was not valid when all soil categories were considered together. However, when fitted to each category, the RMS error on moisture estimates ranged from 2.0% to 3.5% except for silty soils with crusting problems (6%). Results also indicated that, when the soils have similar colors (i.e. same hue), soil categories can be partly grouped and the model can be simplified, using the same intercept coefficients. This study has potential application for the definition of a more generalized model of the soil reflectance. It shows that the impact of soil moisture on reflectance could be higher than differences in reflectance due to the soil categories.

## 1. Introduction

Deriving soil moisture from spectral data has important application in agriculture and in hydrology. Early studies on soil samples in laboratory conditions showed that the reflectance at all wavelengths in the range $0.4-2.5$ μm decreased as the moisture content increased (Bowers & Hanks, 1965; Hoffer & Johannsen, 1969). This general trend was first modeled by Skidmore, Dickerson, and Shimmelpfennig (1975), with oven-dry soil samples at the wavelength of 1.95 μm. The authors considered that wavelengths other than highly moisture-sensitive ones could be used as well. However, deriving soil moisture from remote sensing data remains rather difficult, as the reflectance of a soil is not just a function of moisture but is affected by intrinsic soil factors: amount of organic matter, particle size distribution, mineral composition, and color of soil elements (Escadafal, Girard, & Courault, 1989; Hoffer & Johannsen, 1969; Hovis, 1966; Mattikalli, 1997; Stoner & Baumgardner, 1981). Moreover, as the penetration of the signal in the soil is small, disturbances in the superficial layer or in the roughness of the soil aggregates modify soil reflectance (Boissard, Pointel, Renaux, & Begon, 1989; Cierniewski, 1987; Courault, 1989). In the laboratory, soil structure is generally destroyed prior to reflectance measurement on samples, and in the field, soil structure is variable and continuously modified by farm works or by the climate. In addition, crop residues or active vegetation may drastically disturb the spectral responses of soils or prevent a direct observation. Reflectance of soils depends also on the sun–target–sensor geometry. Jaquemoud, Baret, and Hanocq, (1992) developed in the laboratory the SOILSPEC radiative transfer model that accounts for both the soil roughness, the solar–view angle geometry, and the intrinsic optical properties of soils materials to compute soil bidirectional reflectance from 450 to 2450 nm. One of the model's parameters, the single scattering albedo, $\omega$, is independent of soil roughness and measurement conditions (sun and view angles), and depends only of the intrinsic optical properties of soil material in a given wavelength. Jaquemoud et al. (1992) showed that $\omega$ decreases with soil moisture, but their data set was not sufficient to propose a model that describe the effect of soil moisture on $\omega$.

The penetration of the signal is better in the thermal infrared and in the microwave domains and both domains have in some circumstances a better potential for monitoring the soil moisture (Davidson & Watson, 1995; Engman,

1991; Schmugge, 1980, 1984; Vlcek & King, 1983). Recent models tested for the retrieval of soil moisture using LOTREX airborne radar (Schmullius & Furrer, 1992), AIR-SAR (Lin, Wood, Beven, & Saatchi, 1994), or SIR-C (Wang, Hsu, Shi, O'Neill, & Engman, 1997), gave encouraging results over bare soils but not on moderately or densely vegetated areas. Clearly, any spectral domain (e.g. reflectance, thermal or microwave) has its own limitations and no one is used to predict routinely soil moisture. However, the reflectance domain is the most operational one, as images are easily available at a broad range of ground resolutions. Several studies provide solutions for estimating soil moisture using reflectance images, Digital Elevation Models, Geographic Information Systems and specific classification algorithms (Avila, Yoshiba, Evangelista, & Rondal, 1994; Lindsey, Gunderson, & Riley, 1992; Shih & Jordan, 1992). However, methods are often based on the distribution of landcover classes, rather than on the reflectance of soils. Spectral mixture analysis has also been proposed to extract from heterogeneous landscapes information on each component (Borel & Gerstl, 1994; García-Haro, Gilabert, & Meliá, 1996). In such algorithms, reference spectra for soils are often considered as stable or unique, and the effect of moisture on the spectra not included in the models because it is not known. In the literature, there is a lack of studies on the modeling of soil moisture using reflectance data.

The present study aims at modeling the relationships between soil moisture in real field situation and the corresponding soil reflectance in images. It was assumed that a model could be properly identified on bare soils only (i.e. on plots without vegetation), and that, in such restricted conditions, the variation in reflectance could be attributed to soil moisture only. In other words, disturbing factors in the field plots such as small crop residues and local microtopographic irregularities were considered as residual in the model. The important issues were therefore the timing for an efficient observation of soil moisture, the identification of the model in optimum conditions and the variation of the model with the soil type and the ground resolution.

## 2. Time window for an effective reflectance of soil moisture

We showed previously (Muller & James, 1994) that the underlying soil spectral structure of a landscape, usually masked by the vegetation cover, could be revealed by specific and stable soil spectral patterns and best identified in a time series of TM images when the dominant crops are being sowed. Over the Garonne Valley, France, a multidate composite image was created from several single images acquired on distinct springs in order to concentrate the information on bare soils (more than 75% of the area could be analyzed using six images). In the process, image data were normalized using a method based on pseudo-invariant objects (Muller, 1993). The classification of the composite image provided a good partition of the study area into four broad soil texture categories: clay, silt, silty clay, and sand. These results suggested that the most appropriate period for analyzing the soil moisture–reflectance relationships should be when the subsurface structure of the soil is made homogeneous and without vegetation following synchronized preparations for sowing crops (e.g. in Europe, in winter for wheat and rapeseed, in spring for maize and sunflower). In the Garonne Valley, the optimum time window corresponds, each year, to the end of April beginning of May, i.e. when the dominant spring crops are sowed. This was confirmed by a preliminary test made over an area of $4 \times 4$ km, big enough for observing the four contrasted soil categories but small enough for the soils to receive the same rainfall. Soil moisture content was measured every 10 days, from February to May on 13 sites, with two replicates per site, distant of about 30 m. Results showed that surface soil moisture evolved similarly to the rainfall and that there was no significant difference between soil categories except on the beginning of May ($P < .001$ at the 5% confidence level) when the soil surface structure became homogeneous following synchronized field preparations for the sowing. At the preceding dates, soil surface roughness was made heterogeneous by the plow of February or March. At the end of May and later, the soil structure was homogeneous but the young seedlings were increasingly growing and direct observation of soils was difficult.

## 3. Modeling the soil moisture–reflectance relationships in optimum conditions

### 3.1. Method

On May 6, 1993, images were acquired from a special airborne mission using a Push Broom RAMI sensor of the Centre National d'Etudes Spatiales (CNES) onboard the Avion de Recherche Atmosphérique et de Télédétection (ARAT) aircraft. The study area was a section of 50 km along the Garonne Valley in order to observe a broad range of soil moistures in each soil category. The RAMI sensor was primarily designed for the simulation of the XS1, XS2, and XS3 bands of the SPOT $1-2$ and 3 satellites (i.e. without the shortwave infrared band). Data were geometrically and radiometrically corrected using the absolute calibration coefficients and the flight parameters, and were further simulated at six geometric resolutions (i.e. 5, 10, 15, 20, 25, and 30 m) in the three SPOT bands using the averaging method of Marceau, Gratton, Fournier, and Fortin (1994). Atmospheric corrections were made using the 5 S model (Tanré et al., 1986).

Potential sites for simultaneous moisture measurements and reflectance analysis were identified during the days preceding the flight mission and reported on a topographic map at the scale of 1:25,000. Selected sites should meet two conditions: (1) to be a large agricultural field recently
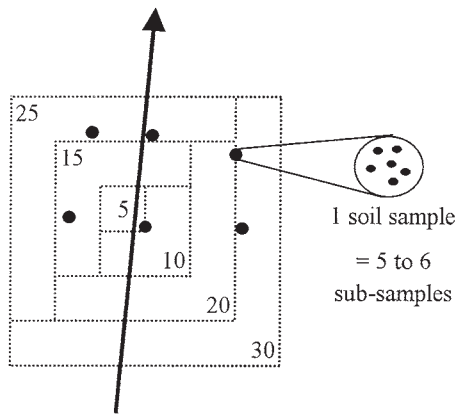
Fig. 1. Field sampling method for soil moisture measurements. At each site, six soil samples were taken at distances of about 5 to 10 m, i.e. two samples along the presumed flight line (black arrow), two samples on the left and two samples on the right. Dotted lines show (possible) positions for the six nested pixels extracted over the site with spatial resolutions of 5, 10, 15, 20, 25, and 30 m, respectively.

prepared for sowing and therefore uniformly bare, and (2) to be located strictly at the vertical of the planned flight line in order to avoid anisotropic disturbances in the scanning directions of the sensor. On this basis, in addition to the absence of clouds, no more than 59 sites could be selected over 50 km. 'Randomness' of site selection was assumed on the basis of the unpredictability of both the site location and the cultivation practice along independent flight lines as well as of a strict exhaustive selection of the sites along each flight line. Each site was further affected into one of the four broad soil categories, i.e. clay, silt, silty clay, and sand, according to the previous classified image (Muller & James, 1994).

Four teams of three operators went to the field during the flight mission (i.e. between 10 a.m. and 1 p.m.). They collected soil samples on each site located on the maps. Six soil samples per site were taken at an approximate distance of 5 to 10 m each, i.e. two samples along the track, two samples on the right and two samples on the left (Fig. 1). Local variability within 1 to 2 m$^2$ was integrated by mixing in each sample five to six subsamples. Each sample of about half of a kilogram of soil was collected from the very superficial millimeters of the soil, using a metallic scraper, and were closed in a hermetic plastic box and weighted. The boxes were opened in the laboratory and dried in an oven at 105°C during 24 h. A drying test over 3 days showed that 24 h allowed obtaining stable dry weights. Boxes with dry soils were then weighted and the corresponding soil moisture was computed as percentage of dry soil weight. For control purposes, the field operators had also to draw quickly, on each site, a sketch map showing the locations of the six soil samples and indicating the view points and directions of at least two photographs taken with a standard 24 × 36 mm camera. This information was crucial for better locating each sampling site in the image. A third picture was taken vertically to provide information on the superficial structure of the soil.

## 4. Results

### 4.1. Variation of soil moisture and reflectance

The surface soil moisture ranged from 1.9% to 32.4% of dry soil weights over the 59 random sites (Fig. 2a). Such an exceptional large range of soil moisture followed very localized rains during the 48 h before the flight mission,
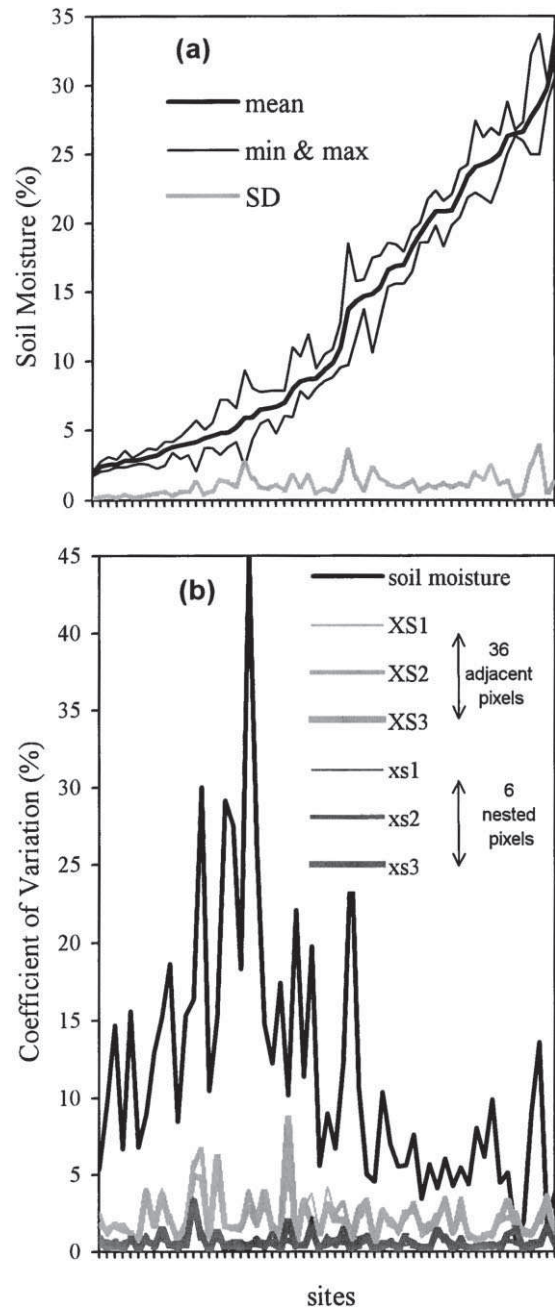


Fig. 2. Local variation of soil moisture and reflectance over the 59 sites, ranked by increasing order of mean moisture. (a) Mean moisture value and standard deviation (S.D.) are plotted together with the minimum and the maximum within-site moisture value. (b) The CV computed by site for the soil moisture (over the six samples), and for the reflectance in bands XS1, XS2, and XS3 (over the six nested pixels and the 36 adjacent pixels).
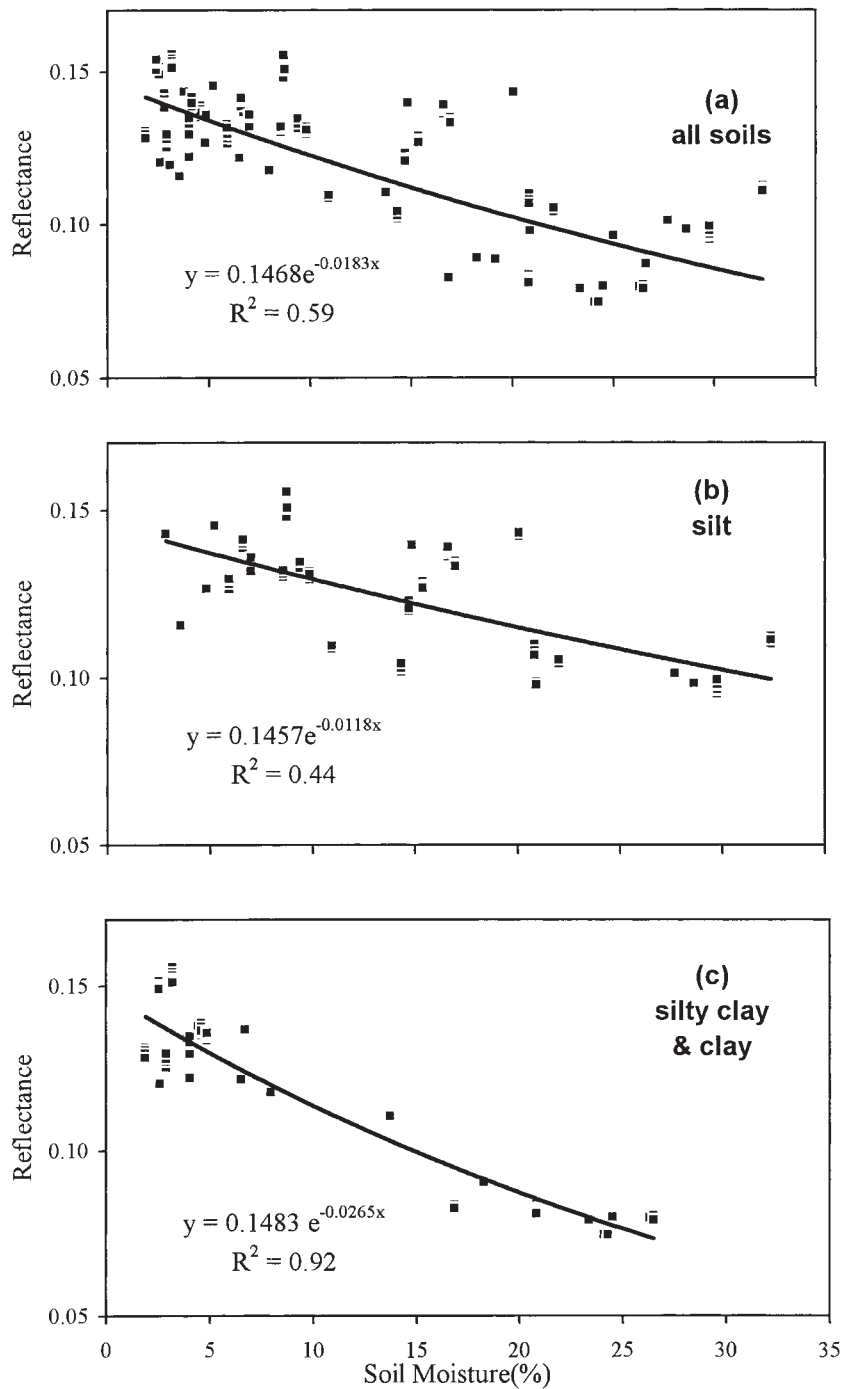
Fig. 3. Exponential regression of the reflectance in XS1 on the soil moisture, over 59 points for all soil categories, 27 points for silt, and 23 points for silty clay and clay.

including early showers on the day of the flight. The local variation of soil moisture, computed for each site by the standard deviation (S.D.) over the six independent soil samples collected by site, fluctuated from 0.1% to 3.9%. It only exceeded 2% on five sites where the local surface irregularities were slightly higher than in other sites. The mean value of the S.D. over the 59 sites was 1.1% (0.95% when the five heterogeneous sites were excluded). Therefore, on average, soil moisture remained rather homoge-

neous within a site (S.D. ∼1%), and no pattern of increasing or decreasing S.D. with increasing moisture was observed.

Each site was characterized by two sets of reflectance data: (1) six strongly dependent nested pixels, respectively of 5, 10, 15, 20, 25, and 30 m resolution, and (2) the 36 adjacent 5-m pixels included in a pixel of 30 m and presumed independent. For comparisons between the two sets of data and between these two sets and the correspond-

ing variation of soil moisture, the unitless coefficient of variation (CV) was computed within each site as the ratio of the standard deviation by the mean value. Obviously, all CV did not have the same meaning, but together they could provide an indication on the range of local variation (Fig. 2b). As expected, the range of variation of reflectance was slightly higher with the 36 adjacent pixels than with the six nested pixels. Little difference was observed from one spectral band to the other. The CV of reflectance remained very low over the 59 sites, never exceeding 4% (mean 0.6%) over six nested pixels and 9% (mean 2%) over 36 adjacent pixels whatever the site or the spectral band. Such results clearly indicate a strong local homogeneity of the reflectance within a pixel of 30 m and strong redundancies between spectral bands. In contrast, soil moisture CV fluctuated from 0.6% to 45%, with a mean close to 11% (i.e. 6 to 20 times higher than reflectance CV). Moreover,

## XS1

**intercept coefficients** $\rho_{so(\lambda)}$

| | | | |
|---|---|---|---|
| sand | 0.1472 | | |
| | | 0.1479 | |
| clay | 0.1399 | | 0.1479 |
| | | 0.1483 | |
| silty-clay | 0.1486 | | 0.1468 |
| | | 0.1420 | |
| silt | 0.1457 | | |

**reflectance attenuation factor** $a_{s(\lambda)}$

| | | | |
|---|---|---|---|
| sand | -0.0201 | | |
| | | -0.0248 | |
| clay | -0.0241 | | -0.0248 |
| | | -0.0265 | |
| silty-clay | -0.0256 | | -0.0183 |
| | | -0.0109 | |
| silt | -0.0118 | | |

**coefficients of determination** $R^2$

| | | | |
|---|---|---|---|
| sand | 0.86 | | |
| | | 0.88 | |
| clay | 0.83 | | 0.89 |
| | | 0.92 | |
| silty-clay | 0.67 | | 0.59 |
| | | 0.44 | |
| silt | 0.44 | | |

**RMS error in the moisture estimate (%)**

| | | | |
|---|---|---|---|
| sand | 3.5 | | |
| | | 3.7 | |
| clay | 2.6 | | 3.3 |
| | | 2.5 | |
| silty-clay | 2.0 | | 6.0 |
| | | 6.0 | |
| silt | 6.4 | | |

Fig. 4. Comparison of parameters in exponential models obtained for different soil categories by regressions of reflectance in XS1 on soil moisture. RMS errors were computed for inverse models using soil moisture as the dependent variable.

## XS2

**intercept coefficients** $\rho_{so(\lambda)}$

| | | | |
|---|---|---|---|
| sand | 0.1836 | | |
| | | 0.1844 | |
| clay | 0.1696 | | 0.1853 |
| | | 0.1875 | |
| silty-clay | 0.1866 | | 0.1850 |
| | | 0.1782 | |
| silt | 0.1853 | | |

**reflectance attenuation factor** $a_{s(\lambda)}$

| | | | |
|---|---|---|---|
| sand | -0.0233 | | |
| | | -0.0294 | |
| clay | -0.0279 | | -0.0296 |
| | | -0.0322 | |
| silty-clay | -0.0293 | | -0.0211 |
| | | -0.0121 | |
| silt | -0.0135 | | |

**coefficients of determination** $R^2$

| | | | |
|---|---|---|---|
| sand | 0.84 | | |
| | | 0.87 | |
| clay | 0.85 | | 0.89 |
| | | 0.93 | |
| silty-clay | 0.66 | | 0.57 |
| | | 0.45 | |
| silt | 0.50 | | |

**RMS error in the moisture estimate (%)**

| | | | |
|---|---|---|---|
| sand | 4.4 | | |
| | | 3.9 | |
| clay | 2.4 | | 3.4 |
| | | 2.3 | |
| silty-clay | 2.1 | | 6.1 |
| | | 6.1 | |
| silt | 6.2 | | |

Fig. 5. Continuation for XS2.

soil moisture CV were lower on moist soils (6%) than on dry soils (12%), the two types of soils being separated by a soil moisture of 15%. Therefore, modeling the soil moisture–reflectance relationships on dry soil is de facto more difficult than on wet soils.

### 4.2. Soil moisture–reflectance relationships

The general trend of decreasing reflectance with increasing moisture was not clearly observed in the soil moisture–reflectance relationships in combining all soil sites together (Fig. 3a). Exponential models, provided slightly better regressions than linear models but coefficients of determination ($R^2$) never exceeded .59 whatever the spectral band considered. Results could not be improved by using the three spectral bands in a multilinear regression or by changing the geometric resolution. In the plot diagrams, the length of each dot in the Y-axis corresponds to the range of variation of the reflectance within the six nested pixels

## XS3

**intercept coefficients $\rho_{so(\lambda)}$**

| sand | 0.2970 | | | |
| clay | 0.2839 | 0.3000 | 0.3028 | |
| | | 0.3069 | | 0.3054 |
| silty-clay | 0.3011 | 0.2947 | | |
| silt | 0.3098 | | | |

**reflectance attenuation factor $a_{s(\lambda)}$**

| sand | -0.0172 | | | |
| clay | -0.0237 | -0.0238 | -0.0241 | |
| | | -0.0268 | | -0.0166 |
| silty-clay | -0.0205 | -0.0081 | | |
| silt | -0.0105 | | | |

**coefficients of determination $R^2$**

| sand | 0.72 | | | |
| clay | 0.79 | 0.80 | 0.84 | |
| | | 0.92 | | 0.50 |
| silty-clay | 0.44 | 0.39 | | |
| silt | 0.53 | | | |

**RMS error in the moisture estimate (%)**

| sand | 6.2 | | | |
| clay | 3.2 | 4.9 | 4.2 | |
| | | 3.0 | | 6.6 |
| silty-clay | 2.2 | 6.6 | | |
| silt | 5.6 | | | |

Fig. 6. Continuation for XS3.

extracted over the site. This indicates that the influence of the spatial resolution of images is negligible on the models.

Assuming that soil reflectance varies not only with soil moisture but also primarily with soil type, regressions were computed by soil category. Again, exponential models provided better regression fits than the linear models. There was no significant difference in fit between spectral bands and no improvement with multilinear regression using the three spectral bands. However, important differences were noted from one soil category to the other. In Figs. 4–6, the comparison of the coefficients of determination showed that the best exponential regressions for a single category were obtained with sand or clay. The poorest results were with silt and silty clay.

According to our results, the general model for moisture–reflectance relationships is as follows (Eq. (1)):

$$\rho_{s(\lambda)} = \rho_{so(\lambda)}\exp(a_{s(\lambda)}M) \qquad (1)$$

where $\rho_{s(\lambda)}$ is the reflectance of the wet soil s in the spectral band $\lambda$, $a_{s(\lambda)}$ is the reflectance attenuation factor for the soil s in the spectral band $\lambda$ due to the soil moisture $M$, and $\rho_{so(\lambda)}$ is the theoretical reflectance of the soils in the spectral band $\lambda$, with a soil water content at air dryness.

Regression models using the soil moisture as the dependent variable had similar $R^2$ coefficients and RMS errors in the estimation of soil moisture ranging between 2.3% and 6.6%, depending on the category of soil and the spectral band (Figs. 4–6). The poorest precision was obtained with all soil categories together or with silty soils. Results also indicate that the soil categories may be partly combined without degrading the model. The precision of the model was 3.3% and 3.4% with XS1 and XS2, respectively, when silty soils were excluded.

## 5. Discussion

The local variation in soil moisture, at the site level, was rather low in terms of standard deviation (mean S.D. $\sim 1\%$ over 59 sites). However, the CV for soil moisture was up to 20 times higher than for the reflectance. As already mentioned by Foody (1991), difficulties exist for the determination of 'true' soil moisture in the field, especially as no instrument can measure the soil moisture content within a micrometer or less (i.e. the probable penetration depth in the reflectance domain). Little could be expected for modeling the relationships between soil moisture and reflectance when considering all soil categories together. Soil texture must be considered as a driving factor for modeling the soil moisture, and each soil category is better characterized by its own specific model.

In this study, the models were developed in optimum conditions, including the artificial (but uncontrolled) homogenization of the surface soil structure by the farmers, i.e. almost simultaneously using similar machines. In modern farming, soil preparation for sowing is very uniform and



Fig. 7. In the simplified exponential model, attenuation coefficients vary with the soil categories and with the spectral bands, while the intercept is the same.

potential difference on superficial soil structure due to difference in soil texture is considerably reduced. Difference may rather exist from one farmer to another or even from one field to another, depending on the orientation of the very small ridges and furrows. Such uncontrolled variations were considered as residual in the models.

The main difference between the models was in the attenuation factor $a_{s(\lambda)}$, rather than in the $Y$-axis intercept $\rho_{so(\lambda)}$. The $\rho_{so(\lambda)}$ coefficients were very similar. This suggests a simplified model (Fig. 7) using the same $Y$-axis intercepts $\rho_{o(\lambda)}$ for all soil categories, in a spectral band $\lambda$ (Eq. (2)):

$$\rho_{s(\lambda)} = \rho_{o(\lambda)} \exp(a_{s(\lambda)} M) \qquad (2)$$

The approximation $\rho_{so(\lambda)} \approx \rho_{o(\lambda)}$ can be justified by the homogeneity of the colors of the soils in the study area. In the Munsell color chart, soils are described by three parameters: hue, value, and chroma (Munsell Color, 1975). The hue notation relates to primary colors, the value to lightness, and the chroma to strength. In this study, the colors of the soils were very close. They had the same hue (2.5Y), with values ranging from 4/ to 6/ and chroma from /3 to /4. Clay soils were dark grayish brown/olive brown (2.5Y 4/3) or olive brown/light olive brown (2.5Y 4.5/4), sandy soils were light olive brown (2.5Y 5/4) or light yellowish brown (2.5Y 6/4), and silty soils were light yellowish brown (2.5Y 6/4). According to Escadafal et al. (1989), increasing clay and moisture content in soils decreases value (and chroma) but does not modify the hue. The unity in the hue of the soils in the Garonne Valley can probably be explained by the fact that soils have a similar origin. The valley is characterized by large subhorizontal geomorphologic units (i.e. Pleistocene terraces and Holocene deposits in the floodplain) and alluvial deposits came from the same area in the Pyrenees. As a consequence, all possible combinations of soil elements do not actually exist. Therefore, when soils have a similar origin and have evolved under similar constraints, they may have the same hue and therefore be modeled using the same constant $\rho_{o(\lambda)}$. In the models, the reflectance attenuation factors $a_{s(\lambda)}$ due to the soil moisture characterizes each soil category specifically. As noted, when two or three soil categories are grouped together (silt excepted), the models remain rather good (Fig. 4). It also is of importance that this study revealed very small differences between exponential and linear models. This suggests that linear models can be accepted as good approximations of the exponential models, at least over a limited range of moisture.

In this study, images were acquired between 10 a.m. and 1 p.m., and the measurements sites were samples at the vertical of the flight lines. In other words, the effect of the sun−soil−sensor geometry on the reflectance was not considered. As mentioned, this effect was addressed by Jaquemoud et al. (1992), who developed a more general soil reflectance model, the SOILSPEC radiative transfer model. In the laboratory, they analyzed 26 soils in 42 different view angles with five simulated TM bands, but for only three moisture levels. Therefore, they considered that future studies should try to relate the single scattering albedos $\omega_\lambda$ to the soil moisture content. Our soil moisture−reflectance model based on field data and airborne images gives indication on the type of relationships that could be used in the SOILSPEC model.

## 6. Conclusion

Our study shows that there exists a relationship between soil moisture in the field and reflectance data in images. Therefore, the limitation of using reflectance data for quantifying soil moisture should not be attributed to the absence of such relationships. It can be analyzed and modeled if remote sensing data are acquired in a favorable time window, which varies with the study area. Our study provides a general method to analyze and model the reflectance changes due to soil moisture in real field situations. The proposed two-parameter exponential model has a simple but universal structure. As any model, it needs to be fitted to local situations in order to determine the locally valid parameters for the model. Once the model is known, it can be further integrated in coupled soil and vegetation radiative transfer models, in spectral unmixing algorithms or in classification approaches. It may therefore facilitate extraction of information in mixed soil-vegetated areas. The model may even have more potential applications on natural ecosystems with low percentage vegetation cover than on agricultural areas, due to changes in soil surface structure with farm works in the case of crops.

Our results indicate that:

(1) The efficiency of the individual spectral bands SPOT XS1, XS2, and XS3 are very similar, and band combinations do not improve the models.

(2) In a fluvial landscape characterized by large and uniform subhorizontal units, the models can be considered as robust for a ground resolution varying from 5 to 30 m.

(3) Best models are exponential, but linear models are good approximations. Models are more efficient when computed by soil category, but the efficiency remained when soils are partly grouped excluding silt soils: soil moisture can be estimated with a mean error of 3.3%.

(4) In the proposed models, the intercept $\rho_{so(\lambda)}$ is representative of the specific hue of the soil (i.e. of intrinsic stable soil characteristics) and the reflectance attenuation factors $a_{s(\lambda)}$ characterizes the impact of soil moisture on the reflectance changes with each soil category.

(5) The reflectance seems to be a poor indicator of the soil moisture when soils are dry (i.e. with moisture below 10%).

(6) When soil moisture varies from 30% to $\sim$0%, reflectance may increase up to 100%, while differences in reflectance due to soil categories only remain within a 50%

variation. This situation clearly shows that subtle reflectance variations due to intrinsic soil parameters can be masked by changes in soil moisture.

## Acknowledgments

## References

Avila, V. E., Yoshiba, M., Evangelista, M. A. M., & Rondal, J. L. (1994). A methodology for soil moisture condition detection using remotely sensed data. *Asian Pacific Remote Sensing Journal*, *7* (1), 109–118.

Boissard, P., Pointel, J. G., Renaux, B., & Begon, J. C. (1989). Zonage et quantification de la stabilité structurale de sols cultivés basés sur des données du satellite Landsat-TM, Application au cas d'une parcelle d'orge en Beauce. *Comptes Rendus de l'Academie des Sciences Paris, Série II: Pédologie*, *309*, 145–152.

Borel, C. C., & Gerstl, S. A. W. (1994). Nonlinear spectral mixing models for vegetative and soil surfaces. *Remote Sensing of the Environment*, *47*, 403–416.

Bowers, S. A., & Hanks, R. J. (1965). Reflection of radiant energy from soils. *Soil Science*, *2*, 130–138.

Cierniewski, J. (1987). A model for soil surface roughness influence on the spectral response of bare soils in the visible and near-infrared range. *Remote Sensing of the Environment*, *23*, 97–115.

Courault, D. (1989). *Etude de la dégradation des états de surface du sol par télédétection, analyses spectrales, spatiales et diachroniques.* p. 237. Paris: Collection Sols, Institut National Agronomique.

Davidson, D. A., & Watson, A. I. (1995). Spatial variability in soil moisture as predicted from Airborne Thematic Mapper (ATM) data. *Earth Surface Processes*, *20*, 219–230.

Engman, E. T. (1991). Applications of microwave remote sensing of soil moisture for water resources and agriculture. *Remote Sensing of the Environment*, *25*, 213–226.

Escadafal, R., Girard, M. C., & Courault, D. (1989). Munsell soil color and soil reflectance in the visible spectral bands of Landsat MSS and TM data. *Remote Sensing of the Environment*, *27*, 37–46.

Foody, G. M. (1991). Soil moisture content ground data for remote sensing investigations of agricultural regions. *International Journal of Remote Sensing*, *12*, 1461–1469.

García-Haro, F. J., Gilabert, M. A., & Meliá, J. (1996). Linear spectral mixture modelling to estimate vegetation amount from optical spectral data. *International Journal of Remote Sensing*, *17*, 3373–3400.

Hoffer, R. M., & Johannsen, J. (1969). Ecological potentials in spectral signature analysis. In: P. L. Johnson (Ed.), *Remote sensing in ecology*. Athens University of Georgia Press Athens (Georgia, USA) (Chapter 1).

Hovis, W. A., Jr. (1966). Infrared spectral reflectance of some common minerals. *Applied Optics*, *5*, 245–248.

Jaquemoud, S., Baret, F., & Hanocq, J. F. (1992). Modeling spectral and bi-directional soil reflectance. *Remote Sensing of the Environment*, *41*, 123–132.

Lin, D. S., Wood, E. F., Beven, K., & Saatchi, S. (1994). Soil moisture estimation over grass-covered areas using AIRSAR. *International Journal of Remote Sensing*, *15*, 2323–2343.

Lindsey, S. D., Gunderson, R. W., & Riley, J. P. (1992). Spatial distribution of point soil moisture estimates using Landsat TM data and fuzzy-c classification. *Water Resources Bulletin*, *28* (5), 865–875.

Marceau, D. J., Gratton, D. J., Fournier, R. A., & Fortin, J. P. (1994). Remote sensing and the measurement of geographical entities in a forested environment: 2. The optimal spatial resolution. *Remote Sensing of the Environment*, *49*, 105–117.

Mattikalli, N. M. (1997). Soil color modeling for the visible and near-infrared bands of Landsat sensors using laboratory spectral measurements. *Remote Sensing of the Environment*, *59*, 14–28.

Muller, E. (1993). Evaluation and correction of angular anisotropic effects in multidate Spot and Thematic Mapper data. *Remote Sensing of the Environment*, *45*, 295–309.

Muller, E., & James, M. (1994). Seasonal variation and stability of soil spectral patterns in a fluvial landscape. *International Journal of Remote Sensing*, *9*, 1885–1900.

Munsell Color. (1975). *Munsell soil color charts*. Baltimore, MD: Macbeth Division of Kollmorgen.

Schmugge, T. J. (1980). Survey of methods for soil methods estimation. *Water Resources Research*, *16*, 961–979.

Schmugge, T. J. (1984). Microwave remote sensing of soil moisture. In: *Proceedings of the 11th international symposium on remote sensing of environment* ( pp. 859–875). Ann Arbor, MI: ERIM.

Schmullius, C., & Furrer, R. (1992). Some critical remarks on the use of C-band radar data for soil moisture detection. *International Journal of Remote Sensing*, *17*, 3387–3390.

Shih, S. F., & Jordan, D. D. (1992). Landsat mid-infrared data and GIS in regional surface soil-moisture assessment. *Water Resources Bulletin*, *28* (4), 713–719.

Skidmore, E. L., Dickerson, J. D., & Shimmelpfennig, H. (1975). Evaluating surface-soil water content by measuring reflectance. *Soil Science Society of America Proceedings*, *39*, 138–242.

Stoner, E. R., & Baumgardner, M. F. (1981). Characteristic variations in reflectance of soils. *Soil Science Society of America Journal*, *45*, 1161–1165.

Tanré, D., Deroo, C., Duhaut, P., Herman, M., Morcrette, J. J., Perbos, J., & Deschamps, P. Y. (1986). *Simulation of the satellite signal in the solar spectrum (5 S)*. Lille: Laboratoire d'Optique Atmospherique, Université des Sciences et des Techniques (148 pp.).

Vlcek, J., & King, D. (1983). Detection of subsurface soil moisture by thermal sensing: results of laboratory, close-range and aerial studies. *Photogrammetric Engineering and Remote Sensing*, *49* (11), 1593–1597.

Wang, J. R., Hsu, A., Shi, J. C., O'Neill, P. E., & Engman, E. T. (1997). A comparison of soil moisture retrieval models using SIR-C measurements over the Little Washita River watershed. *Remote Sensing of the Environment*, *59*, 308–320.